^{1}H MR Spectroscopy in Cervical Carcinoma using External Phase Array Body Coil at 3.0 Tesla: Prediction of Poor Prognostic Human Papillomavirus Genotypes

Gigin Lin MD, PhD,[1,2]* Chyong-Huey Lai MD,[3] Shang-Yueh Tsai PhD,[4] Yu-Chun Lin PhD,[1] Yu-Ting Huang MD,[1] Ren-Chin Wu MD, PhD,[5] Lan-Yan Yang PhD,[6] Hsin-Ying Lu MS,[1,2] Angel Chao MD, PhD,[3] Chiun-Chieh Wang MD, PhD,[7] Koon-Kwan Ng MD,[1] Shu-Hang Ng MD,[1] Hung-Hsueh Chou MD,[3] Tzu-Chen Yen MD, PhD,[8] and Ji-Hong Hung MD, PhD[7]

Purpose: To assess the clinical value of proton (^{1}H) MR spectroscopy in cervical carcinomas, in the prediction of poor prognostic human papillomavirus (HPV) genotypes as well as persistent disease following concurrent chemoradiotherapy (CCRT).
Materials and Methods: ^{1}H MR spectroscopy using external phase array coil was performed in 52 consecutive cervical cancer patients at 3 Tesla (T). Poor prognostic HPV genotypes (alpha-7 species or absence of HPV infection) and persistent cervical carcinoma after CCRT were recorded. Statistical significance was calculated with the Mann-Whitney two-sided nonparametric test and areas under the receiver operating characteristics curve (AUC) analysis.
Results: A 4.3-fold ($P = 0.032$) increased level of methyl resonance at 0.9 ppm was found in the poor prognostic HPV genotypes, mainly attributed to the presence of HPV18, with a sensitivity of 75%, a specificity of 81%, and an AUC of 0.76. Poor prognostic HPV genotypes were more frequently observed in patients with adeno-/adenosquamous carcinoma (Chi-square, $P < 0.0001$). In prediction of the four patients with persistent disease after CCRT, elevated methyl resonance demonstrated a sensitivity of 100%, a specificity of 74%, and an AUC of 0.82.
Conclusion: ^{1}H MR spectroscopy at 3T can be used to depict the elevated lipid resonance levels in cervical carcinomas, as well as help to predict the poor prognostic HPV genotypes and persistent disease following CCRT. Further large studies with longer follow up times are warranted to validate our initial findings.
Level of Evidence: 1

J. MAGN. RESON. IMAGING 2017;45:899–907.

Cervical cancer is the third most common cancer in women worldwide,[1] with estimated new cases and deaths of 12,990 and 4120, respectively, in the United States in 2016.[2] Human papillomavirus (HPV), a well-established causative factor for cervical cancer, has shown to impact on prognosis.[3–8] For patients undergoing primary

View this article online at wileyonlinelibrary.com. DOI: 10.1002/jmri.25386

Received May 23, 2016, Accepted for publication Jun 28, 2016.

*Address reprint requests to: G.L., 5 Fuhsing Street, Guishan, Taoyuan, Taiwan 33382. E-mail: giginlin@cgmh.org.tw

From the [1]Department of Medical Imaging and Intervention, Institute for Radiological Research, Chang Gung Memorial Hospital at Linkou and Chang Gung University, Guishan, Taoyuan, Taiwan; [2]Clinical Phenome Center, Chang Gung Memorial Hospital at Linkou, Guishan, Taoyuan, Taiwan; [3]Department of Obstetrics and Gynecology and Gynecologic Cancer Research Center, Chang Gung Memorial Hospital at Linkou and Chang Gung University, Guishan, Taoyuan, Taiwan; [4]Graduate Institute of Applied Physics, National Chengchi University, Wenshan District, Taipei, Taiwan; [5]Department of Pathology, Chang Gung Memorial Hospital at Linkou and Chang Gung University, Guishan, Taoyuan, Taiwan; [6]Clinical Trial Center, Chang Gung Memorial Hospital at Linkou and Chang Gung University, Guishan, Taoyuan, Taiwan; [7]Department of Radiation Oncology, Chang Gung Memorial Hospital at Linkou and Chang Gung University, Guishan, Taoyuan, Taiwan; and [8]Department of Nuclear Medicine and Center for Advanced Molecular Imaging and Translation (CAMIT), Chang Gung Memorial Hospital at Linkou, Guishan, Taoyuan, Taiwan

Additional supporting information may be found in the online version of this article.

concurrent chemoradiotherapy (CCRT), the presence of alpha-7 species or absence of HPV infection results in a poorer prognosis, as compared with tumors infected by alpha-9 species or multiple HPV infection.[3–5] In early-stage cervical cancer undergoing primary surgery, large cohort studies demonstrated that HPV18 positivity is significantly related to cancer relapse and disease-specific death in invasive cervical cancers.[6,7] On the other hand, HPV16-negativity is proven to be a significant poor prognostic factor in cervical adenocarcinoma or adenosquamous carcinoma (AD/ASC).[8]

The International Federation of Gynecology and Obstetrics (FIGO) incorporated cross-sectional imaging into the evaluation and treatment planning in its 2009 version, demonstrating the increasing importance of medical imaging in the management of cervical cancer.[9] Among the imaging armamentarium, MR imaging has been proven to be useful in staging of cervical carcinomas of FIGO stage IB1 or greater,[10] supported by its accuracy for evaluating tumor size,[11] detecting parametrial invasion,[12] and a high negative predictive value for excluding bladder and rectal invasion.[13] Furthermore, reductions of disease-free survival rate are associated with presence of bulky tumor size[14] or deep stromal invasion in clinical stage IB disease.[15,16]

In additional to anatomical information on MR imaging, proton (^{1}H) MR spectroscopy can provide insights into tumor biochemistry. The clinical usefulness of ^{1}H MR spectroscopy has been established for central nervous system disorders,[17] such as brain neoplasms, demyelinating disorders, and infectious brain lesions. With the improvement of MR scanners and increased field strength, the list of applications includes the assessment of aggressiveness for prostate cancer,[18] the detection of lipid dysregulation in the breast cancer of women carrying BRCA1 and BRCA2 genetic mutations.[19] Prior studies have demonstrated the use of MR spectroscopy in detection of lipid alterations, which are common in cervical cancer.[20–22] Whether lipid alterations on MR spectroscopy might further differentiate poor prognostic HPV genotypes and potentially impact on patient management, however, has not been exploited.

The aim of this study is to assess the clinical values of ^{1}H MR spectroscopy in prediction of poor prognostic HPV genotypes in cervical carcinoma.

Materials and Methods

Patients

Our Institutional Review Board approved this prospective study and informed consent was obtained. The study setting was in a tertiary referral center with a dedicated interdisciplinary gynecological oncology team. From July 2013 to December 2014, gynecological MR exams were prospectively conducted for a consecutive series of 60 patients with histologically proven and untreated cervical cancer who were scheduled to receive primary surgery or chemoradiation therapy. The inclusion criteria for this study were: biopsy proven treatment naïve cervical cancer with clinical visible lesion, i.e., FIGO IB and above; estimated tumor size > 1.5 cm determined by clinical pelvic exam; patients must be ≥ 20 of age; patients must be willing to undergo standard treatment such as surgery or chemoradiation therapy; patients must be able to give informed consent. The exclusion criteria were: patients who are judged to be noncompliant to treatment or not accessible for follow-up; patients with contraindications to MR scanning, such as claustrophobia, cardiac pacemaker, metal implants in field of view, or unable to cooperate for MR study due to mental status. In the data verification phase, we excluded three patients of endometrial carcinoma with cervical extension.

Medical records of eligible patients were identified and centrally reviewed in the weekly interdisciplinary meeting before enrolment, to ensure the study quality. Clinical parameters including tumor histology, differentiation, clinical FIGO stage and major methods of treatments were recorded. The outcomes of patients who underwent CCRT were followed up at least for 1 year.

MR IMAGING. Enrolled patients were imaged with a 3 Tesla (T) MR system (Skyra, Siemens, Erlangen, Germany). The lower nine elements of the integrated spine coil and the lower six element of the body-phased array coil were used to study the entire pelvis.[23] T2-weighted (5630/87; average, 3; matrix, 256×320; FOV, 20 cm) and diffusion-weighted (DW) MR imaging using single-shot echo-planar technique with fat suppression (repetition time ms/echo time ms, 3300/79; number of signal average, 4; section thickness, 4 mm; gap 1 mm; matrix, 128×128; field of view 20×20 cm) were performed. The diffusion-weighted gradients were applied orthogonally in slice-selective, phase encoding and read out directions. Apparent diffusion coefficient (ADC) maps were generated from isotropic DW images, with b value of 0 and 1000 s/mm^2, by calculating the slope of the logarithmic decay curve for signal intensity against b value (Syngo, Siemens, Erlangen, Germany). Sequences were obtained in identical slice thickness and gaps for both T2W and DWI, in the axial and sagittal planes to cover the entire true pelvis. Intravenous bolus injection of 0.1 mmol/kg body weight of contrast medium (gadopentetate dimeglumine, Magnevist, Schering, Berlin, Germany) was carried out in routine exams but not for study purpose. Study patients were encouraged to control their minimal free breathing during MR exams. No premedication was administered. Two radiologists (Y.T.H. and G.L., with 8 and 10 years of experience in gynecological radiology, respectively) evaluated the maximal diameter and mean ADC value of tumors on the workstation, blinded to the spectroscopic results. The location (exocervix or endocervix) and morphology (infiltrating or lobulated) of each lesion was recorded.

MR SPECTROSCOPY. Triplane localizer 1D MRS with point-resolved spectroscopy (PRESS) was performed by selecting a $12 \times 12 \times 12$ mm3 spectroscopic volume prescribed by gynecological radiologists (Y.T.H. and G.L.). Volume of interests were placed within the cervical tumor (high signal intensity tumor area on high-b-value DW and low ADC, to prevent the influence of fluid in cervical canal and/or tumor post biopsy), free of adipose tissue (as seen on T1 and T2-weighted images), necrotic area or Nabothian cysts (as seen on T2-weighted images), and large arteries (as

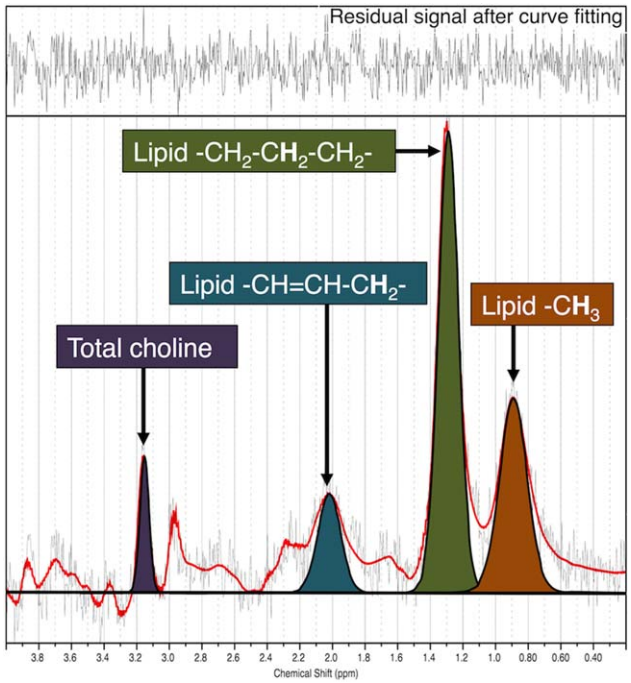

FIGURE 1: Representative ^{1}H-MR spectrum. Lipid resonances δ 0.9 ppm (methyl, $-CH_3$), δ 1.3 ppm ($-CH_2-CH_2-CH_2-$), δ 2.0 ppm $-CH=CH-CH_2-$), and total choline resonance δ 3.2 ppm were quantified using LCModel software (Provencher, Ontario, CA).

seen on T1-weighted images). The B0 shimming parameters were optimized with a free-breathing rapid B0 mapping method. For each voxel placement, automated optimization of gradient shimming was performed. The water line width within the PRESS box was measured following shimming, and if the value was greater than 15 Hz, the PRESS box was repositioned and re-shimmed or spectroscopy was abandoned. B0 maps (dual gradient-echo; repetition time [TR] 50 ms; echo tmes [TEs] 7.6 and 17.6 ms) were obtained after shimming, before MR spectroscopic acquisition to ensure there were no significant susceptibility artifacts or B0 inhomogeneity. The following parameters were used: TR/TE, 2000 ms/35 ms; 128 averages; vector size, 1024 points; bandwidth, 1200 Hz. Water suppression was achieved using band selective inversion with gradient dephasing. Nonwater suppressed spectra as concentration references were also measured with the same scan parameters, except acquiring only four signal averages to reduce scan time to 16 s. A total scan time for MR spectroscopy was approximately 7 min, integrated in routine MR imaging sessions. The reason of using an external coil rather than an endovaginal coil was to minimize the invasiveness of procedure and to integrate MR spectroscopy in routine pelvic examination.

MR SPECTROSCOPY ANALYSIS. MR spectroscopy data were analyzed using the LCModel software (version 6.3–0 K; Provencher, Ontario, CA, Canada) on a Linux workstation, and eddy current correction was performed. Spectra were phased and multiplied by the complex conjugate of the reference water spectrum. LCModel automatically integrated resonance amplitudes for lipids (fatty acyls at 0.9 ppm, 1.3 ppm, and 2.0 ppm) and choline (3.2 ppm), using the corresponding water signals as a reference. It was not possible to measure metabolite relaxation times in each patient, so no correction for relaxation was included. The Cramer-Rao lower bound (CRLB) value, which simultaneously accounts for both line width and signal to noise ratio, was calculated as an estimate of the error in metabolite quantification. MR spectra were excluded if CRLB value of methyl resonance at 1.3 ppm exceeded the 30% range. A representative MR spectrum is shown in Figure 1.

Histopathology

Cervical carcinoma tissues were obtained from surgical specimens during standard operations or punch biopsy in the patients undergoing chemoradiation therapy. Histopathologic types and tumor differentiations were evaluated in consensus of a general pathologist and a specialized gynecological pathologist (R.C.W.). If the primary site of tumor was uncertain, an additional immunohistochemical study was performed to exclude the possibility of endometrial cancer and confirm the diagnosis of cervical cancer.

HPV Genotyping

Poor prognostic HPV genotypes were defined as alpha-7 species (HPV18, 39, 45) and absence of HPV infection in this study, as opposed to favorable prognostic alpha-9 species (HPV16, 31, 33, 52, 58) and multiple HPV genotypes.[3] The procedure for the HPV genotyping has been reported previously.[3,8,24] Briefly, DNA was extracted from paraffin embedded specimens and amplified by polymerase chain reaction for the L1 open reading frame with biotinylated GP6 + and SPF1 consensus primers. Resultant amplifiers were hybridized with the Easychip® HPV Blot membranes (King Car, Taiwan), which were then incubated with Avidex streptavidin-alkaline phosphatase conjugate and developed color with NBT/BCIP (nitro-blue tetrazolium chloride/5-bromo-4-chloro-3′-indolyphosphate p-toluidine) to determine the final HPV genotypes, in which 38 types of HPV could be detected. Type-specific polymerase chain reaction (PCR) reactions were performed to validate multiple types and HPV-negativity on HPV Blot. In case of discordance between results, a repeat of HPV Blot, SPF1/GP6 + PCR and direct sequencing were performed to resolve the discrepancy.[24,25]

Statistical Analysis

Data were analyzed using MedCalc for Windows, Version 9.2.0.0 (MedCalc Software, Mariakerke, Belgium). Bland-Altman test was computed to examine the variability between repeated MR spectroscopy measurements for the first 10 subjects to test the reproducibility of this study. Continuous variables were analyzed with the Mann-Whitney U test (two-group comparisons). Pearson's Chi-square was used to evaluate the association between the presence of HPV infection and histology type of squamous cell carcinoma (SCC) or AD/ASC. Areas under the receiver operating characteristics curve (AUCs) were applied to compare performances of MR spectroscopy in differentiating HPV prognostic genotypes, histopathology, and tumor response to chemoradiation. The sensitivity, specificity and diagnostic accuracy were represented with 95% confidence interval (CI). $P < 0.05$ was considered to indicate a significant difference.

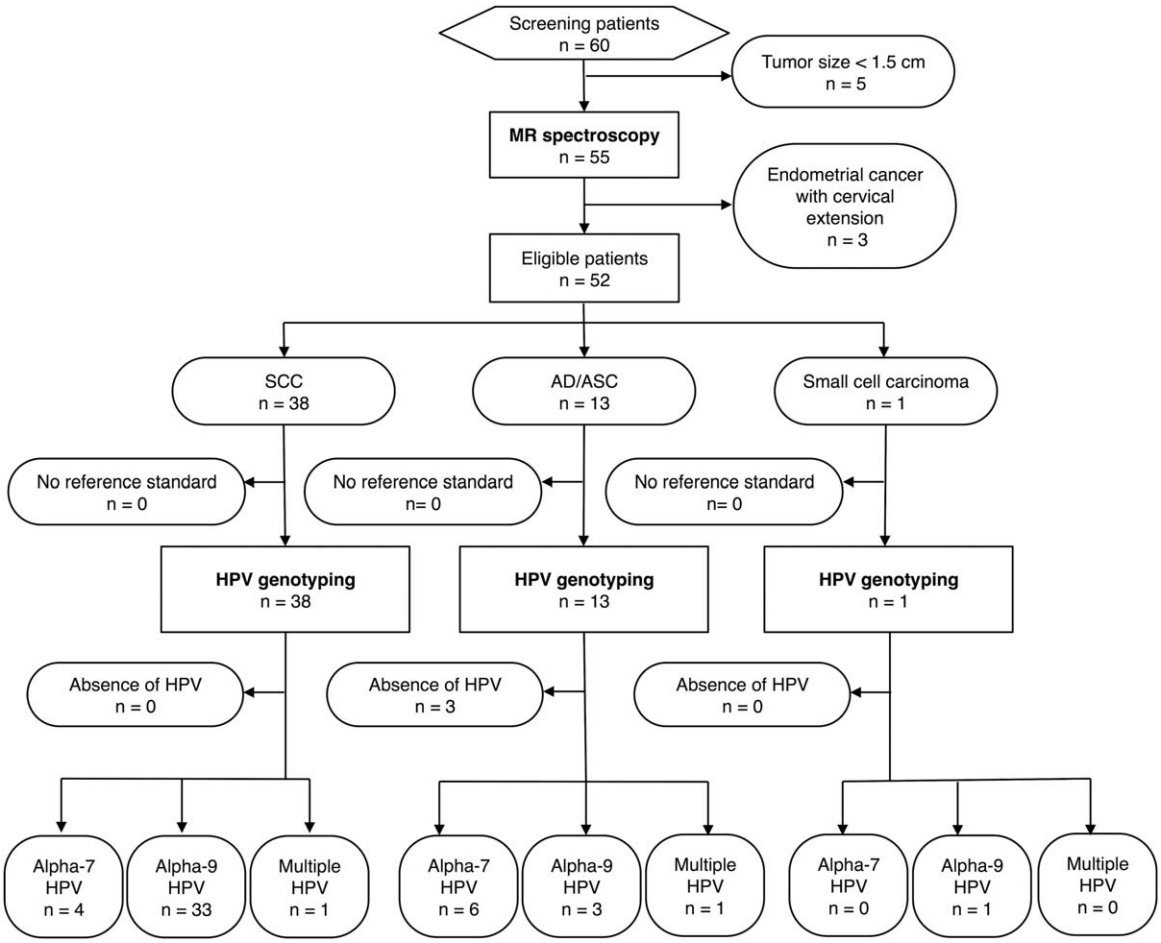

FIGURE 2: Flow diagram of study cohort.

Results

Patient Demographics and Reproducibility

The flow diagram of study cohort is demonstrated in Figure 2. Fifty-two patients (age range, 27–88 years; median age, 52 years) entered the data analysis. Fourteen patients underwent surgical hysterectomy and 38 patient received punch biopsy and concurrent chemoradiation. The patient demographics is summarized in Table 1. Bland-Altman plots demonstrated differences within mean ± 1.96 standard deviation (SD) in our first 10 enrolled subjects and confirmed the reproducibility of this study (Supp. Fig. S1, which is available online). MR spectroscopy was carried out without report any discomfort or adverse event.

Differentiating Prognostic HPV Genotypes

Comparison between the HPV groups showed a 4.3-fold ($P = 0.032$) increased level of methyl resonance at 0.9 ppm in the patients with poor prognostic HPV genotypes. Similar trends of increase in methyl resonance at 0.9 ppm related to poor prognostic HPV genotypes were found in the subgroup analysis, with a 1.6-fold ($P = 0.292$) increase and a fivefold ($P = 0.273$) in SCC group and AD/ASC group, respectively. A 5.2-fold ($P = 0.042$) increase in the methyl resonance was noticed in the patients infected with HPV18, as compared with HPV16 (Figs. 3 and 4) (Table 2). Resonances from methylene at 1.3 pm, unsaturated lipid at 2.0 ppm, as well as total choline at 3.2 ppm, demonstrated increased levels in poor prognostic HPV group, albeit not statistically significant. With an optimal methyl resonance threshold of greater than 144, the AUC was 0.76 (95% CI: 0.57–0.90), in differentiating poor and favorable prognostic HPV genotypes (Table 3), a sensitivity of 75% and a specificity of 81%, and an odds ratio (OR) of 12.75 (95% CI: 1.84–88.36). Using the same threshold, the AUC of methyl resonance was 0.82 (95% CI: 0.55–0.96) in differentiating HPV18 and HPV16 (Fig. 5), with a sensitivity of 83% and a specificity of 90%, in discriminating HPV18 and HPV16 (OR, 45, 95% CI: 2.29–885.65). No significant differences in tumor ADC values were found between the poor and favorable HPV prognostic groups (mean ± SD, 92 ± 12 versus $87 \pm 18 \times 10^{-5}$ mm^2/s, $P = 0.122$), which reflected on a low AUC of 0.65 (95% CI: 0.34–0.75), a sensitivity of 69% and a specificity of 64%.

Differentiating Histological Types

Fourfold and 3.5-fold ($P = 0.028$ for both) elevated levels of methyl resonance at 0.9 ppm and methylene resonance at

TABLE 1. Patient Demographics[a]

Variable	Data (n = 52)
Age, median (y)	52 (27-80)
Tumor size, median (cm)	4 (1.5-10)
Histopathology	
Squamous cell carcinoma	38
Adenocarcinoma	11
Adenosquamous carcinoma	2
Small cell carcinoma	1
Differentiation	
Well, moderate	32
Poor	17
Undetermined	3
HPV	
Alpha-7	
18	10
Alpha-9	
16	20
31	2
33	9
52	2
58	4
Multiple[b]	2
Absence	3
FIGO stage	
IB	17
IIA	5
IIB	22
IIIA	1
IIIB	5
IV	2
Treatment	
Concurrent chemoradiotherapy	38
Surgery	14

[a]Unless otherwise indicated, data are number of patients, with range in parentheses. HPV = human papillomavirus.
[b]HPV genotypes 16, 33 (n = 1) and HPV genotypes 18, 33 (n = 1).

1.3 ppm were observed in the AD/ASC group, as compared with SCC group (Table 2). Resonances from unsaturated fatty acyl chain at 2.0 ppm, demonstrated a 3.2-fold increase in AD/ASC group, albeit not statistically significant ($P = 0.088$). In comparison of tumors with poorly and moderately/well differentiated tumor grades, no significant difference was identified on MR spectroscopy. The AUC in differentiating AD/ASC and SCC groups based on methyl resonance at 0.9 ppm was 0.77 (95% CI: 0.58–0.90) (Table 3). Tumor ADC value was significantly higher in AD/ASC group as compared with SCC group (mean ± SD, 104 ± 16 versus $85 \pm 11 \times 10^{-5}$ mm^2/s, $P < 0.0001$). Poor prognostic HPV genotypes were more frequently observed in patients with histology types of AD/ASC (Chi-square, $P < 0.0001$). No difference was found between SCC and AD/ASC groups in terms of their location (exocervix versus endocervix, $P = 0.411$) and morphology (infiltrating versus lobulated, $P = 0.930$).

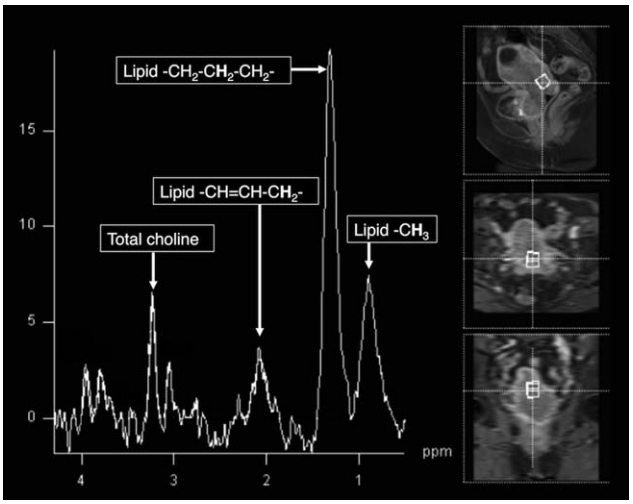

FIGURE 3: MR spectroscopy of a 61-year-old woman with cervical adenocarcinoma and HPV18 infection. FIGO IIB, tumor size 4 cm.

Lipid Alterations in Prediction of Persistent Tumor After CCRT

Thirty-eight patients underwent concurrent chemoradiation therapy. In prediction of the four patients with persistent tumor, elevated methyl resonance at 0.9 ppm on

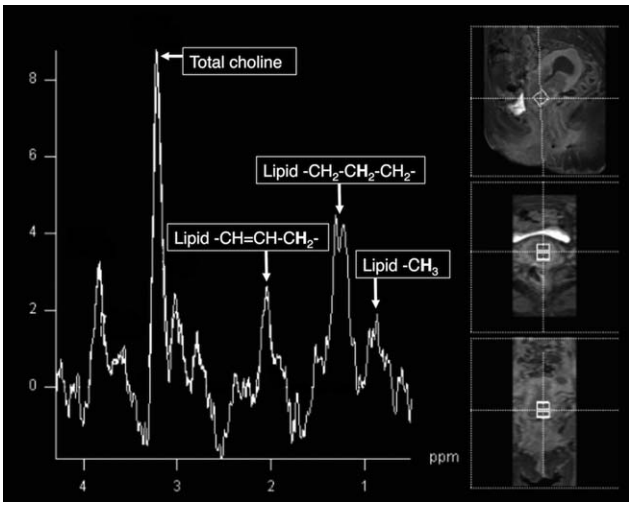

FIGURE 4: MR spectroscopy of a 50-year-old woman with cervical squamous cell carcinoma and HPV16 infection. FIGO IIB, tumor size 4.5 cm.

TABLE 2. Alterations of Lipid Resonances in Various Risk Groups[a]

Poor prognostic HPV genotypes	Present (n = 13)	Absent (n = 39)	*P*-Value
Lipid -CH3, δ 0.9 ppm (mM)	243.37 ± 50.17	97.06 ± 18.76	0.032[a]
Lipid -CH2-CH2-CH2-, δ 1.3 ppm (mM)	780.43 ± 237.42	498.23 ± 100.88	0.333
Lipid -CH=CH-CH2-, δ 2.0 ppm (mM)	115.89 ± 24.84	53.08 ± 8.97	0.093
Total choline, δ 3.2 ppm (mM)	5.32 ± 1.25	3.68 ± 0.62	0.216
Adeno/adenosquamous carcinoma	Present (n = 13)	Absent (n = 38)	
Lipid -CH3, δ 0.9 ppm (mM)	215.45 ± 49.68	107.70 ± 21.01	0.028[a]
Lipid -CH2-CH2-CH2-, δ 1.3 ppm (mM)	1002.63 ± 258.03	410.93 ± 84.07	0.028[a]
Lipid -CH=CH-CH2-, δ 2.0 ppm (mM)	101.95 ± 20.24	58.66 ± 11.19	0.088
Total choline, δ 3.2 ppm (mM)	3.31 ± 1.10	4.38 ± 0.66	0.457
Poor differentiation	Present (n = 17)	Absent (n = 32)	
Lipid -CH3, δ 0.9 ppm (mM)	174.24 ± 42.58	111.44 ± 22.56	0.245
Lipid -CH2-CH2-CH2-, δ 1.3 ppm (mM)	763.26 ± 213.33	498.81 ± 99.43	0.361
Lipid -CH=CH-CH2-, δ 2.0 ppm (mM)	76.92 ± 16.55	74.90 ± 13.58	0.617
Total choline, δ 3.2 ppm (mM)	4.07 ± 0.96	4.29 ± 0.75	0.918

[a]Unless otherwise indicated, data are means ± standard error of mean. *P*-Values were obtained with the Mann-Whitney U test.

pretreatment MR spectroscopy demonstrated a sensitivity of 100% and a specificity of 74%, with an AUC of 0.82 (95% CI: 0.67–0.93), higher than prediction of ADC value (AUC = 0.54; 95% CI: 0.38–0.71). However, the small sample size of persistent disease was statistically insignificant to draw the conclusion ($P = 0.160$).

Discussion

The present study demonstrated that MR spectroscopy using external phase array coils at 3.0T can be integrated into routine clinical practice and scanning workflow for patients with cervical cancer. Single voxel PRESS technique enabled sufficient and highly reproducible signal acquisition for metabolite quantification. The short TE of 35 ms in the present study allowed us to observe metabolites with short T2 relaxation times, in particularly benefit for lipid resonance. Addition nonwater suppressed spectra facilitated the quantification of resonance. With the guidance of diffusion-weighted MR imaging, volume of interests were confidently placed within the cervical tumor (high signal intensity tumor area on high-b-value DW and low ADC), to prevent sampling bias attributed to tumor heterogeneity. This could facilitate technologists be trained to define and place the volume of interests under the supervision of radiologists.

Our report exploits links between poor prognostic HPV genotypes and lipid alterations in cervical carcinoma using in vivo MR spectroscopy. The MR spectroscopy prediction of HPV genotype may be a useful predictive factor

TABLE 3. ROC Curve Analysis of Methyl Resonance (0.9 ppm) in Various Groups

	AUC	Cutoff	Sensitivity (%) [95% CI]		Specificity (%) [95% CI]	
Poor prognostic HPV genotypes	0.76	> 144.01	75	[34–97]	81	[58–95]
HPV18	0.82	> 144.01	83	[36–100]	90	[56–100]
Adeno/adenosquamous carcinoma	0.77	> 40.679	100	[63–100]	52	[30–74]
Poor differentiation	0.63	> 37.877	83	[52–98]	47	[23–72]
Persistent tumour after CCRT	0.82	> 40.679	100	[40–100]	73	[56–87]

ROC = receiver operating characteristic.

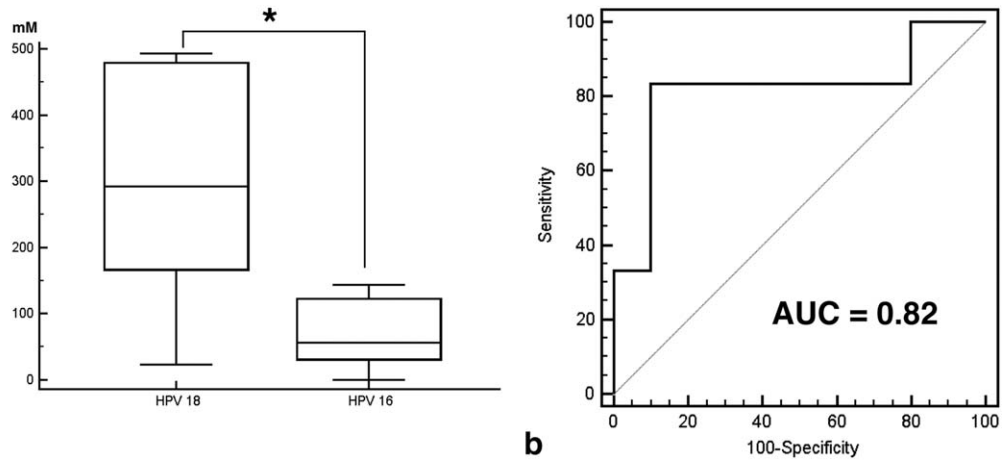

FIGURE 5: Box-and-whisker plot shows a significant lower level of methyl resonance δ 0.9 ppm in HPV18 group, as compared with HPV16 group (a). Receiver operating characteristic (ROC) curve in discriminating HPV 18 versus 16 genotypes. AUC, areas under the ROC curve (b).

for the effect of CCRT in patients with advanced cervical cancer, because concurrent chemoradiation therapy benefits patients with HPV18 or HPV58 more than those with HPV16 or HPV33.[3,4] MR spectroscopy may ultimately help to decrease treatment toxicity while preserving efficacy in this group of patients. In the present study, in vivo MR spectroscopy demonstrated a significantly elevated level of methyl fatty acyl resonance at 0.9 ppm in poorer prognostic HPV genotypes. Concordantly, 0.9-ppm resonance was significantly elevated in HPV18 than in HPV16, the most common types of poor prognostic (alpha-7) and favorable prognostic (alpha-9) species, respectively. Another important lipid resonance, methylene resonance at 1.3 ppm, was reported more commonly elevated in carcinoma in situ (CIN) than normal cervix,[21] with respective a sensitivity of 77% and a specificity of 94% in predicting the presence of cervical carcinoma.[22]

In the present data in differentiation of poorer prognostic HPV genotypes, methylene resonance at 1.3 ppm also demonstrated a trend of elevated level, albeit the difference not statistically significant. Levels of methyl and methylene resonances were greater in the histologically proven AD/ASC group as compared with SCC group, concordant with the fact that HPV18 or alpha-7 species were more commonly presented in AD/ASC rather than SCC.[26] The level of total choline, a mixture of cell membrane phospholipid related metabolites, demonstrated no significantly difference between risk groups in the present study, which was in accordance with a prior report showing no significant difference in choline between any of the tumor histological type, degree of differentiation, presence or absence of lymphovascular invasion, lymph-node involvement, nor between cervical tumor and normal (epithelial or stromal) cervical tissue.[27]

The alteration of in vivo lipid resonances in the present study is supported by prior ex vivo tissue reports.[21,22,28–31] High resolution ex vivo MR spectroscopic analysis of cervical punch biopsy specimens showed that majority biopsy specimens containing dysplastic cells or evidence of HPV infection have a discernible lipid spectrum similar to that of malignant tissue specimens.[28] Ex vivo biopsies have shown levels of methyl and methylene resonances in cervical carcinoma significantly greater than that in normal or CIN biopsies,[21] with a sensitivity of 100% and a specificity of 69% in diagnosis of cancer, independent of the tumor load in the sample.[22] Significant differences in samples containing histologically confirmed cancer were seen for multiple lipid resonances, with an AUC value of 0.96, in detection of cancer in cervical tissue biopsies.[29] The increased methylene level was associated with longer acyl fatty acid side-chain length or less unsaturated in SCC than in normal tissue[30] and correlated with increased numbers of cytoplasmic lipid droplets.[31]

From our preliminary data, the methyl resonance at 0.9 ppm on MR spectroscopy demonstrated potential in prediction of persistent tumors after CCRT and warrants further investigations. Although pretreatment ADC value was reported in differentiation between responders and nonresponders to CCRT,[32] its predictive value remained controversy by the other following reports.[33,34] Nonetheless, data shown here, as well as preliminary reports, demonstrated that the ADC values of primary cervical cancer differed in various histology types,[35,36] which correlated with glucose uptake measured by FDG-positron emission tomography (PET).[37] Taken together, information from MR spectroscopy, DW MR imaging and PET might bring forth aspects into understanding of poor prognostic HPV genotypes, cellularity and glucose metabolism in vivo. In this regard, MR spectroscopy, coupled with anatomical and functional imaging, has potentials to add dimensions of clinical phenotyping.

A limitation to this study was the small number of participants in each category, therefore, we did not correct for multiple comparisons given the exploratory nature of the study. Second, serum lipid levels were not routinely

measured in this study for ethical considerations, although its effect on local tumor tissue was expected to be minimal but cannot be completely excluded. Third, low initial HPV viral load, which was reported to implicate poor prognosis in cervical cancer,[5] was not investigated in the present study. Fourth, the reproducibility of MR spectroscopy requires improvement before this technique becoming widespread application. Furthermore, normal cervical epithelium in patients without cervical cancer was too thin to measure on MR spectroscopy. Hence normal control group was not planned to compare with cervical cancer group. Finally, given a worse survival outcome and increased risks in distant metastasis in patients with AD/ASC, as compared with those with squamous histology,[38–40] caution should be exercised when interprets our data. Because changes on MR spectroscopy were associated with both HPV genotyping and histopathological typing, subgroup analysis to elucidate confounding factors warrants further investigation in the future.

In conclusion, this study demonstrated the feasibility of single voxel MR spectroscopy of cervical carcinoma by using external phase array coil at 3T. We found an elevated level of methyl resonance at 0.9 ppm in the cervical carcinoma with poor prognostic HPV genotypes, as compared with favorable prognostic HPV genotypes. Preliminary data also demonstrated elevation of 0.9-ppm methyl resonances in prediction of persistent tumors after CCRT. MR spectroscopy, coupled with anatomical and functional MR imaging, has potentials to become a robust and integral part of routine MR exam, to add dimensions of clinical phenotyping to guide treatment and outcome prediction for women diagnosed with cervical carcinoma.

Acknowledgment

Contract grant sponsor: Chang Gung Medical Foundation; contract grant number: CMRPG-3B1923; CIRPG3E0021; Contract grant sponsor: National Science Council (Taiwan); contract grant number: NSC103-2314-B-182A-006; IRB No. 102-0620A3; Clinical trial ID: NCT01874548
The authors thank Ms. Chu-Chun Huang for performing HPV genotyping analysis.

References

1. Ferlay J, Soerjomataram I, Dikshit R, et al. Cancer incidence and mortality worldwide: sources, methods and major patterns in GLOBOCAN 2012. Int J Cancer 2015;136:E359–E386.
2. Siegel RL, Miller KD, Jemal A. Cancer statistics, 2016. CA Cancer J Clin 2016;66:7–30.
3. Wang CC, Lai CH, Huang HJ, et al. Clinical effect of human papillomavirus genotypes in patients with cervical cancer undergoing primary radiotherapy. Int J Radiat Oncol Biol Phys 2010;78:1111–1120.
4. Wang CC, Lai CH, Huang YT, Chao A, Chou HH, Hong JH. HPV genotypes predict survival benefits from concurrent chemotherapy and radiation therapy in advanced squamous cell carcinoma of the cervix. Int J Radiat Oncol Biol Phys 2012;84:e499–e506.
5. Kim JY, Park S, Nam BH, et al. Low initial human papilloma viral load implicates worse prognosis in patients with uterine cervical cancer treated with radiotherapy. J Clin Oncol 2009;27:5088–5093.
6. Burger RA, Monk BJ, Kurosaki T, et al. Human papillomavirus type 18: association with poor prognosis in early stage cervical cancer. J Natl Cancer Inst 1996;88:1361–1368.
7. Lai CH, Chang CJ, Huang HJ, et al. Role of human papillomavirus genotype in prognosis of early-stage cervical cancer undergoing primary surgery. J Clin Oncol 2007;25:3628–3634.
8. Lai CH, Chou HH, Chang CJ, et al. Clinical implications of human papillomavirus genotype in cervical adeno-adenosquamous carcinoma. Eur J Cancer 2013;49:633–641.
9. Pecorelli S, Zigliani L, Odicino F. Revised FIGO staging for carcinoma of the cervix. Int J Gynaecol Obstet 2009;105:107–108.
10. Sala E, Rockall AG, Freeman SJ, Mitchell DG, Reinhold C. The added role of MR imaging in treatment stratification of patients with gynecologic malignancies: what the radiologist needs to know. Radiology 2013;266:717–740.
11. Sahdev A, Sohaib SA, Wenaden AE, Shepherd JH, Reznek RH. The performance of magnetic resonance imaging in early cervical carcinoma: a long-term experience. Int J Gynecol Cancer 2007;17:629–636.
12. Sala E, Wakely S, Senior E, Lomas D. MRI of malignant neoplasms of the uterine corpus and cervix. AJR Am J Roentgenol 2007;188:1577–1587.
13. Hricak H, Gatsonis C, Coakley FV, et al. Early invasive cervical cancer: CT and MR imaging in preoperative evaluation - ACRIN/GOG comparative study of diagnostic performance and interobserver variability. Radiology 2007;245:491–498.
14. Burghardt E, Baltzer J, Tulusan AH, Haas J. Results of surgical treatment of 1028 cervical cancers studied with volumetry. Cancer 1992; 70:648–655.
15. Delgado G, Bundy B, Zaino R, Sevin BU, Creasman WT, Major F. Prospective surgical-pathological study of disease-free interval in patients with stage IB squamous cell carcinoma of the cervix: a Gynecologic Oncology Group study. Gynecol Oncol 1990;38:352–357.
16. Zaino RJ, Ward S, Delgado G, et al. Histopathologic predictors of the behavior of surgically treated stage IB squamous cell carcinoma of the cervix. A Gynecologic Oncology Group study. Cancer 1992;69: 1750–1758.
17. Oz G, Alger JR, Barker PB, et al. Clinical proton MR spectroscopy in central nervous system disorders. Radiology 2014;270:658–679.
18. Kobus T, Vos PC, Hambrock T, et al. Prostate cancer aggressiveness: in vivo assessment of MR spectroscopy and diffusion-weighted imaging at 3 T. Radiology 2012;265:457–467.
19. Ramadan S, Arm J, Silcock J, et al. Lipid and metabolite deregulation in the breast tissue of women carrying BRCA1 and BRCA2 genetic mutations. Radiology 2015;275:675–682.
20. De Silva SS, Payne GS, Morgan VA, et al. Epithelial and stromal metabolite changes in the transition from cervical intraepithelial neoplasia to cervical cancer: an in vivo 1H magnetic resonance spectroscopic imaging study with ex vivo correlation. Eur Radiol 2009;19: 2041–2048.
21. Mahon MM, Williams AD, Soutter WP, et al. 1H magnetic resonance spectroscopy of invasive cervical cancer: an in vivo study with ex vivo corroboration. NMR Biomed 2004;17:1–9.
22. Mahon MM, Cox IJ, Dina R, et al. (1)H magnetic resonance spectroscopy of preinvasive and invasive cervical cancer: in vivo-ex vivo profiles and effect of tumor load. J Magn Reson Imaging 2004;19:356–364.
23. Lin G, Ng KK, Chang CJ, et al. Myometrial invasion in endometrial cancer: diagnostic accuracy of diffusion-weighted 3.0-T MR imaging--initial experience. Radiology 2009;250:784–792.
24. Chao A, Jao MS, Huang CC, et al. Human papillomavirus genotype in cervical intraepithelial neoplasia grades 2 and 3 of Taiwanese women. Int J Cancer 2011;128:653–659.

25. Lai CH, Huang HJ, Hsueh S, et al. Human papillomavirus genotype in cervical cancer: a population-based study. Int J Cancer 2007;120: 1999–2006.

26. Clifford G, Franceschi S. Members of the human papillomavirus type 18 family (alpha-7 species) share a common association with adenocarcinoma of the cervix. Int J Cancer 2008;122:1684–1685.

27. Payne GS, Schmidt M, Morgan VA, et al. Evaluation of magnetic resonance diffusion and spectroscopy measurements as predictive biomarkers in stage 1 cervical cancer. Gynecol Oncol 2010;116:246–252.

28. Mountford CE, Delikatny EJ, Dyne M, et al. Uterine cervical punch biopsy specimens can be analyzed by 1H MRS. Magn Reson Med 1990;13:324–331.

29. Zietkowski D, Davidson RL, Eykyn TR, De Silva SS, Desouza NM, Payne GS. Detection of cancer in cervical tissue biopsies using mobile lipid resonances measured with diffusion-weighted (1)H magnetic resonance spectroscopy. NMR Biomed 2010;23:382–390.

30. Mahon MM, deSouza NM, Dina R, et al. Preinvasive and invasive cervical cancer: an ex vivo proton magic angle spinning magnetic resonance spectroscopy study. NMR Biomed 2004;17:144–153.

31. Zietkowski D, deSouza NM, Davidson RL, Payne GS. Characterisation of mobile lipid resonances in tissue biopsies from patients with cervical cancer and correlation with cytoplasmic lipid droplets. NMR Biomed 2013;26:1096–1102.

32. Liu Y, Bai R, Sun H, Liu H, Zhao X, Li Y. Diffusion-weighted imaging in predicting and monitoring the response of uterine cervical cancer to combined chemoradiation. Clin Radiol 2009;64:1067–1074.

33. Zhang Y, Chen JY, Xie CM, et al. Diffusion-weighted magnetic resonance imaging for prediction of response of advanced cervical cancer to chemoradiation. J Comput Assist Tomogr 2011;35:102–107.

34. Kim HS, Kim CK, Park BK, Huh SJ, Kim B. Evaluation of therapeutic response to concurrent chemoradiotherapy in patients with cervical cancer using diffusion-weighted MR imaging. J Magn Reson Imaging 2013;37:187–193.

35. Liu Y, Bai R, Sun H, Liu H, Wang D. Diffusion-weighted magnetic resonance imaging of uterine cervical cancer. J Comput Assist Tomogr 2009;33:858–862.

36. Kuang F, Ren J, Zhong Q, Liyuan F, Huan Y, Chen Z. The value of apparent diffusion coefficient in the assessment of cervical cancer. Eur Radiol 2013;23:1050–1058.

37. Ho KC, Lin G, Wang JJ, Lai CH, Chang CJ, Yen TC. Correlation of apparent diffusion coefficients measured by 3T diffusion-weighted MRI and SUV from FDG PET/CT in primary cervical cancer. Eur J Nucl Med Mol Imaging 2009;36:200–208.

38. Park JY, Kim DY, Kim JH, Kim YM, Kim YT, Nam JH. Outcomes after radical hysterectomy in patients with early-stage adenocarcinoma of uterine cervix. Br J Cancer 2010;102:1692–1698.

39. Lee YY, Choi CH, Kim TJ, et al. A comparison of pure adenocarcinoma and squamous cell carcinoma of the cervix after radical hysterectomy in stage IB-IIA. Gynecol Oncol 2011;120:439–443.

40. Galic V, Herzog TJ, Lewin SN, et al. Prognostic significance of adenocarcinoma histology in women with cervical cancer. Gynecol Oncol 2012;125:287–291.